Plasma position and elongation regulation at FTU using dynamic input allocation

L. Boncagni, S. Galeani, G. Granucci, G. Varano, V. Vitale, L. Zaccarian.

Abstract

In this paper we employ and extend the dynamic allocation theory first presented in [13] to guarantee asymptotic tracking of a prescribed elongation of the plasma cross section in the Frascati Tokamak Upgrade (FTU). This task is hard to accomplish because it can only be achieved using the so-called F poloidal coil, a high bandwidth actuator needed to perform high performance horizontal plasma position regulation. Another actuator, the V poloidal coil, could be used for this positioning task, but its bandwidth is insufficient. Using dynamic input allocation it is possible to hierarchically achieve the two goals above by way of a nonlinear scheme suitably exploiting the two actuators: the high priority (fast) goal is the horizontal position regulation task, while the low priority (slow) goal is the elongation regulation. We present theoretical results supporting the proposed scheme, as well as simulations and experiments showing the effectiveness of the proposed solution.

I. Introduction

The extra degrees of freedom present in systems having more inputs than controlled outputs yield the existence of an infinite choice of the input functions giving rise to the same output response (in particular, at least the same steady state output can be obtained by infinitely many constant input values; hence proper input allocation allows to change the control input without affecting the output, at least asymptotically). While several approaches to input allocation have been proposed for a number of different applications (especially aerospace applications, see e.g. the survey [8], but also underwater vehicles [5] and dual stage actuators in hard disk drives [7]; see also the invited session [2]), their application in the field of nuclear fusion and tokamak plasmas shape control [1] is just starting [11].

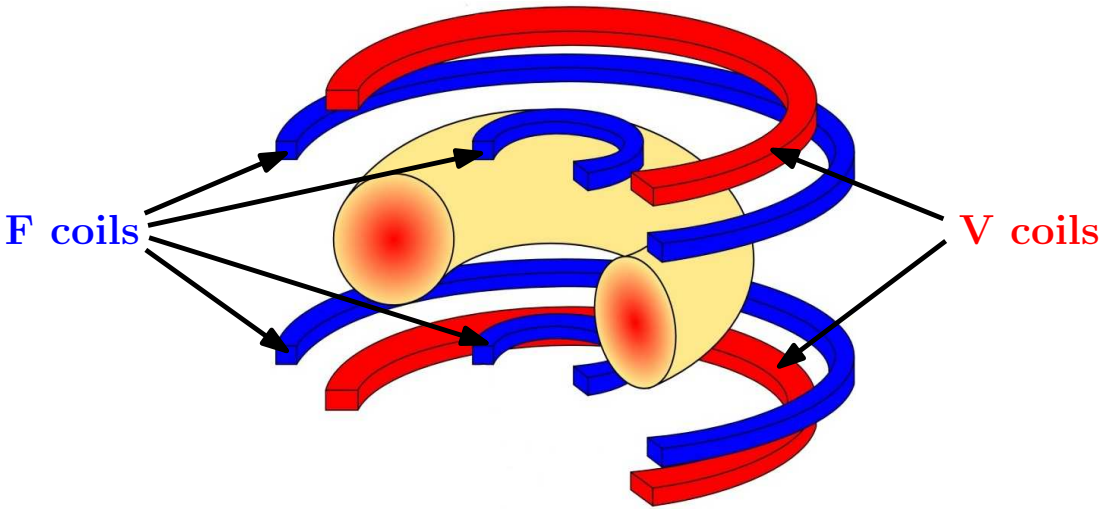

Fig. 1. The F and V coils around the plasma in the Frascati Tokamak Upgrade.

Tokamak plasmas [1], [9], [10] correspond to large scale experimental devices wherein the reaction at the basis of the nuclear fusion phenomenon happening in the stars is studied. Differently from nuclear fission, which involves large atoms and involves breaking them into smaller ones while releasing large amounts of energy arising from the mass loss, in nuclear fusion very small atoms (typically isotopes of hydrogen) are fused together to form heavier ones (typically helium) with a loss of mass which, once again, is capable of releasing large amounts of energy. Reproducing the above reaction on earth is much more difficult than what happens in the stars, because of the lower pressure conditions, which require higher temperatures to increase the probability of a reaction. Tokamaks are the currently preferred technological solution for achieving nuclear fusion on earth, due to their symmetries.

L. Boncagni and V. Vitale are with Associazione Euratom/ENEA sulla fusione, Centro Ricerche Frascati, CP 65 - 00044 Frascati (Roma), Italy
G. Varano, S. Galeani and L. Zaccarian are with the Dipartimento di Informatica, Sistemi e Produzione, Università di Roma "Tor Vergata", 00133 Roma, Italy varano|galeani|zack@disp.uniroma2.it
G. Granucci is with the Associazione EURATOM-CNR sulla Fusione, IFP-CNR, via R. Cozzi 53, 20125 Milano, Italy
Work supported in part by ENEA-Euratom and MIUR.

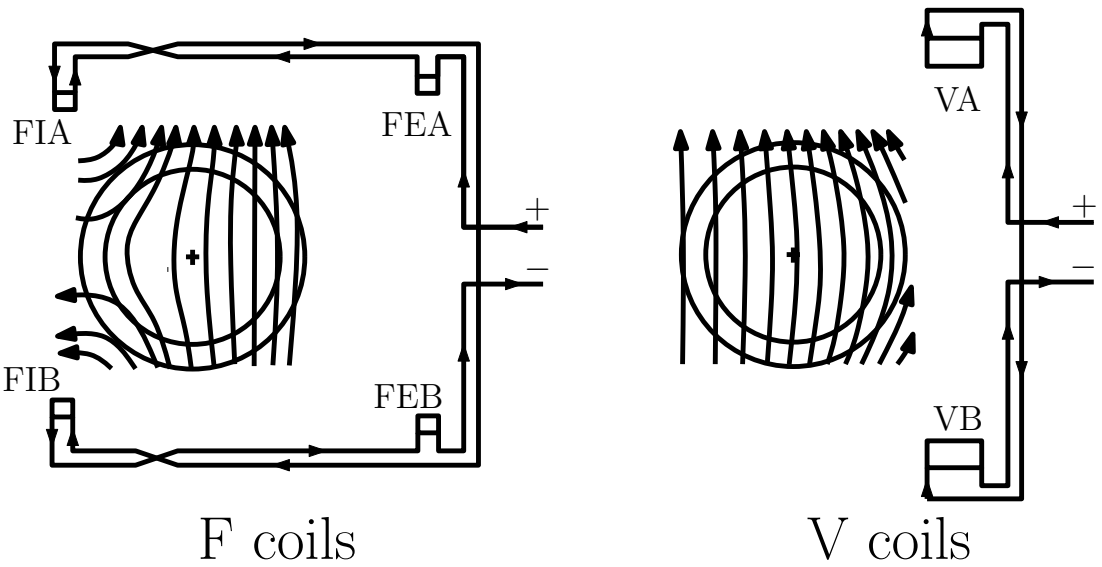

Fig. 2. The magnetic fields generated by the F and V coils on the plasma cross-section.

A tokamak is a toroidal chamber, where the plasma (that is, high temperature matter in a state which is neither solid, gas, nor liquid) is confined by suitable magnetic coils capable of inducing an axialsymmetric configuration, that is, a configuration where any poloidal cross section of the torus looks the same. The primary goal of control of tokamak plasmas is to guarantee suitable positioning of the plasma within the chamber by controlling the current in the magnetic coils. In the Frascati Tokamak Upgrade (FTU), the horizontal positioning system relies on the use of the so-called "V" coil (V standing for "vertical", as it generates a vertical magnetic field which acts on the plasma horizontal position) and "F" coil (F standing for "feedback", as only this coil currently runs in feedback configuration), whose location is shown in the 3D sketch of Figure 1, where the plasma is the donut represented in the center. Due to their toroidal symmetry, the magnetic field generated by the V and F coils is the same on any poloidal section of the plasma and, on that section, it corresponds to the field lines shown in Figure 2. With these field lines, the currents flowing in both the V and the F coils affect the plasma shape, as if the plasma section was a balloon squeezed in between the forces generated by the field. In particular, both the V and the F coils affect the horizontal position of the plasma section (or, more briefly, of the plasma) but the F coil is also capable of slightly compressing the plasma, thus inducing a desirable elongation on it, making it an egg-shaped. In fact, there is a known quasi-static map which well approximates the relationship between the current flowing in the F coil and the elongation (see Section II for more details). Moreover, the two actuators' power supply systems are characterized by different amplitude and rate saturation levels reported in Table I. In fact, the V amplifier can supply large currents, but it has strict current rate limits; on the other hand the F amplifier allows for steeper current profiles, but is more limited in the amplitude range.

coil	Max current [kA]	Max current rate [kA/s]
V	25.0	54
F	12.5	830

TABLE I
AMPLITUDE AND RATE SATURATION LEVELS FOR THE TWO ACTUATORS.

The control system currently used at FTU ensures the regulation of the plasma horizontal position to the requested value, but does not care about its elongation. The horizontal position control (see Figure 3 next) consists of a preprogrammed feedforward action on both the actuators, plus a feedback PID correction through the F coil. The reason why the V coil is not involved in the feedback regulation of the horizontal position is that it is too slow for this crucial task, due to its rate limits. Then, with the control scheme currently used at FTU (before the addition of the elongation controller presented in this paper), the actual current flowing in the F coil during the experiment depends on the PID controller output and therefore on the type of disturbances acting on the experimental system. In most experiments the experience of the physicists leads to a current of roughly 4 kA in the flattop phase, which induces a desirable elongation (typically the vertical axis is $1.03, 1.04$ times larger than the horizontal one). However, any external disturbance that requires a significant action from the PID controller (such as impurities, radiofrequency heating or similar events) causes a significant change in the steady-state current in the F coil and therefore an undesirable elongation. Elongations smaller than 1.03, because of the symmetries, make it difficult to identify certain plasma parameters from the magnetic measurements, thus compromising the plasma equilibrium reconstruction (namely the off-line computation of certain internal parameters of the plasma, often relevant for the physical results of the experiment). One of the many reasons why it is desirable to have an elongation regulation system is maintaining the elongation at sufficiently high values to avoid this reconstruction problem during most of the experimental pulse.

As mentioned above, the only actuator affecting the plasma elongation in FTU is the F coil. However the F coil is necessarily devoted to the high bandwidth plasma horizontal position regulation. Indeed, the V coil (which does affect the plasma horizontal position) is too slow for this task due to its severe rate saturation limits. Nevertheless the slow V coil could be used to slowly take over the F coil effort and make the F coil available for the lower priority task of elongation control which does not require the same bandwidth. Hence, a coordinated action of the two actuators is needed, but classical linear control techniques cannot be used within this setting to guarantee elongation control without resulting in a perturbation for the horizontal position control loop. Moreover with a linear approach the only way to avoid the rate saturation of the V coil is to design a slow enough control, in order to remain inside the bounds also in the worst case, thus resulting in a too conservative solution.

In this paper we employ the dynamic allocation scheme of [13] to combine the action of the V and F coils. From the viewpoint of the horizontal position, the two coils are redundant and can be used to achieve the horizontal regulation goal as a primary task and regulation of the current flowing in the F coil as a secondary task, carried out without perturbing the position loop at all. This secondary task results in ensuring a desired elongation because of the direct relationship between the achieved elongation and the current flowing in the F coil. In particular, once the current in the F coil can be suitably regulated, it is possible to achieve a prescribed desired elongation by suitably inverting the known affine curve relating the F coil current to the corresponding plasma elongation Since elongation regulation is a low priority (low bandwidth) task, very large disturbances would then alter the elongation but only temporarily. In most practical cases, the elongation regulation would be satisfactory. Some preliminary results in the direction pursued here have appeared in [3] and a preliminary and reduced version of this paper can be found in [12].

The paper is organized as follows: in Section II we describe the allocation scheme and give theoretical results, in Section III we give simulation results and in Section IV we describe the experimental results.

II. Dynamic allocation scheme

A. Problem description and solution

For the purpose of this application, the plasma horizontal position behavior during the flat-top phase of the experiments is well described by the simplified model introduced in [14]. A possible state space realization for that transfer function is given by:

$$\begin{aligned} \dot{x} &= Ax + Bu + B_d d, \\ y &= Cx + Du + D_d d, \end{aligned} \tag{1}$$

where x denotes the (unaccessible) internal state of the dynamical model, the control input $u = \left[\begin{smallmatrix} i_V \\ i_F \end{smallmatrix}\right]$ corresponds to the currents requested, respectively, from the V and F coils, the disturbance $d = i_P$ corresponds to the plasma current and the plant output $y = \Delta\Psi$ is an indirect measure of the radial position error (more precisely, it corresponds to the difference between the magnetic flux at the desired radial position and the boundary magnetic flux measured at the limiter point). The system matrices in model (1) are given by:

$$\left[\begin{array}{c|c|c} A & B & B_d \\ \hline C & D & D_d \end{array}\right] = \frac{1}{\tau}\left[\begin{array}{c|cc|c} -1 & k_V & k_F & k_P \\ \hline -1 & k_V & k_F & k_P \end{array}\right], \tag{2}$$

where τ represents the main time constant of the plasma+coils dynamics.

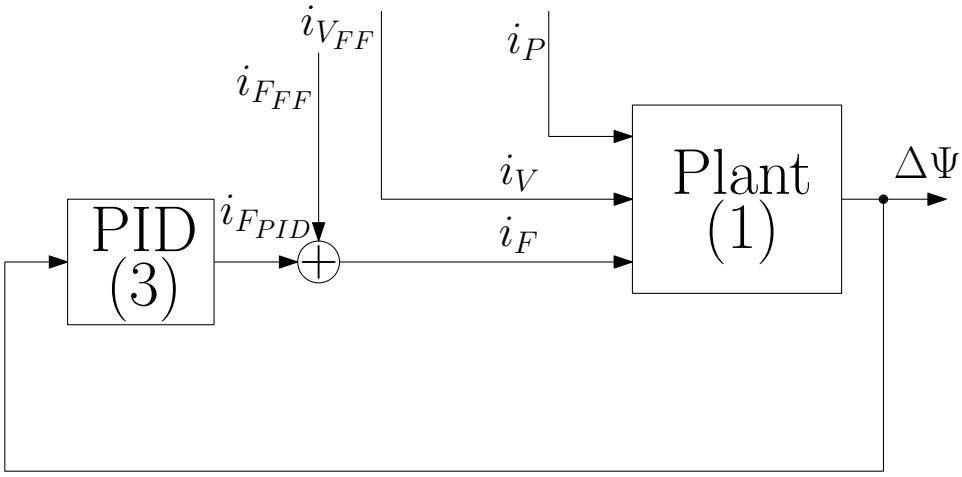

Fig. 3. The current horizontal position regulation scheme. Both the V and F actuators contribute to this task: the V coil is driven by a feedforward action, while the F coil is driven by both a feedforward action and a feedback PID action from the measurement $\Delta\Psi$.

The horizontal position control scheme currently used at FTU, represented in Figure 3, consists in a feedforward action on both the inputs i_V and i_F plus a feedback correction only on i_F, obtained from a PID control. For our purposes the overall

controller can be represented as another generic linear time invariant system of the form:

$$\begin{aligned} \dot{x}_c &= A_c x_c + B_c u_c + B_r r, \\ y_c &= C_c x_c + D_c u_c + D_r r, \end{aligned} \tag{3}$$

where $A_c, B_c, B_r, C_c, D_c, D_r$ are suitable constant matrices, r represents the reference and $y_c = \begin{bmatrix} i_{V_c} \\ i_{F_c} \end{bmatrix}$ is the control signal for the actuators. The controller (3) is connected to the plant (1) as follows:

$$u_c = y, \tag{4a}$$

$$u = y_c, \tag{4b}$$

namely the control is in feedback from the $\Delta\Psi$ measurement and the poloidal currents are driven by the controller (3). The following natural assumption is made, entailing global asymptotic stability of the origin (by the linearity of the system) and existence and uniqueness of the solutions of the feedback interconnection (referred to as well-posedness—see, e.g., [4]).

Assumption 1: The linear closed loop system (1), (3), (4), is well-posed and asymptotically (therefore exponentially) stable.

With the above scenario in place, the goal of this paper is to solve the following input allocation problem:

Problem 1: Given the linear closed-loop system (1), (3), (4) and under Assumption 1, synthesize a nonlinear (possibly dynamic) allocation strategy introducing modification at the plant control input (namely on the current requests for the F and V coils) with the goal of:

1) not introducing any modification on the transient performance induced by the high-bandwidth horizontal regulation task performed by the feedback loop involving the F coil;
2) ensuring low-bandwidth (slow) regulation of the average current flowing in the F coil by effecting a slow input authority transfer from the V to the F coil, exploiting the (weak) input redundancy of the control system;
3) extend the allocation scheme to allow for elongation regulation, making use of the quasi-static (nonlinear) map relating the plasma elongation to the current flowing in the F coil.

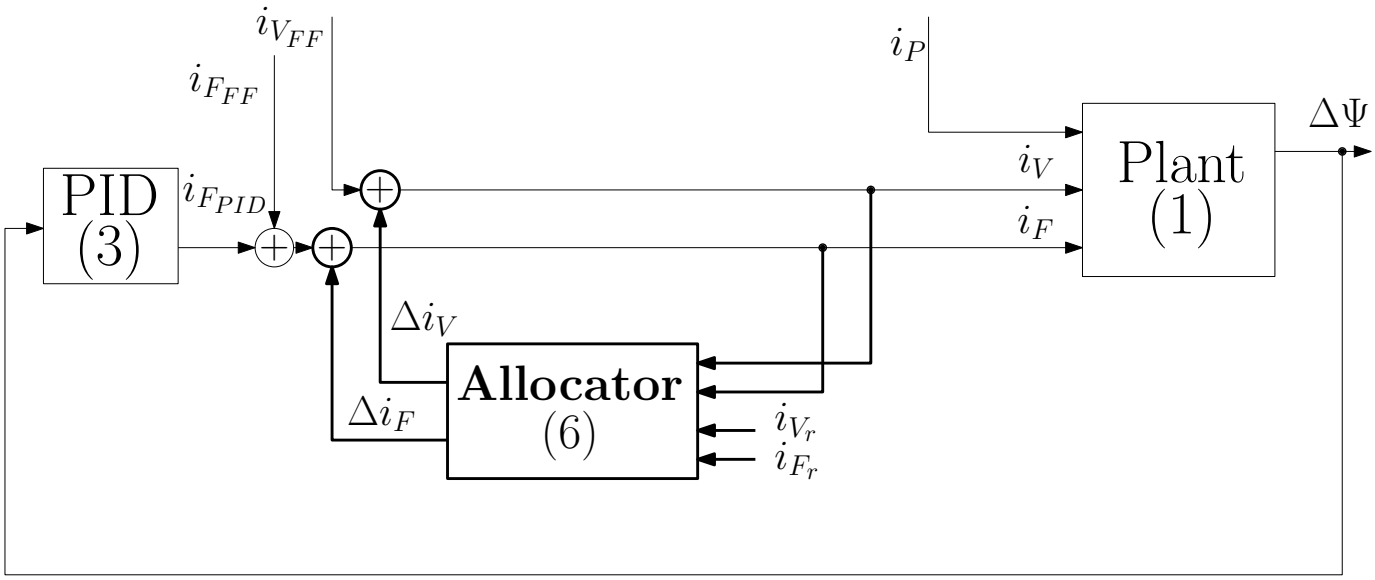

Fig. 4. The dynamic allocator in the closed-loop control scheme.

In Section II-B we will provide a solution to the first two items in Problem 1 by inserting a dynamic allocator block between the controller and the plant of Figure 3, as shown in the scheme of Figure 4. By exploiting the degrees of freedom in the design strategy proposed in [13], and extending the corresponding scheme to the case of time-varying dynamics, we will provide a solution which is capable of exploiting the redundancy only when suitable activation signals are enabled and whenever the modifications $(\Delta i_V, \Delta i_F)$ injected at the plant input are within certain prescribed safety limits. The corresponding scheme, comprising the dynamics in (6), (7), (10) introduced next and interconnected via (8), (9) and with the weight function selection in (11), (12), (13), will solve items 1 and 2 of Problem 1 as formally established in Theorem 1. In particular, it will allow to achieve slow regulation of the current flowing into the F coil to the steady-state reference value given by i_{F_r} in Figure 4, while the transient performance induced by the PID loop will remain essentially unaffected. Finally, to achieve the goal in item 3 of Problem 1, using a suitable inversion of the nonlinear quasi-static map relating the plasma elongation to the current flowing in the F coil, a solution will be given in Section II-C to the plasma elongation regulation problem, which will be accomplished by regulating the F current to a suitable time-varying reference computed from the desired elongation and depending on the plasma current. The formal properties of the arising scheme will be established in Theorem 2.

Remark 1: It should be mentioned that, despite the heavy mathematical derivations, which allow to suitably characterize experimental requirements such as enabling the dynamic allocator action in suitable time windows and ensuring that the

allocator signals and the arising coil currents are below certain prescribed safety limits, the scheme proposed here essentially solves an input allocation problem with redundant actuators, namely the problem of providing a desirable pattern at the input of the plant (that is, the current flowing in the V and F coils), while leaving the plant output performance (that is the plasma horizontal position) essentially unaffected. This type of goal is a quite frequent one in high performance control systems, where specifications on the plant input are given, in addition to specifications on its output. In particular, for tokamak plasmas, a similar scheme is employed to provide input allocation on the JET experiment, with the goal of increasing the available input range in the poloidal field coils, at the price of slightly deteriorating the plasma shape [11]. For general application fields the scheme here proposed can be directly employed in any application where a control task can be performed by two actuators: a large one which is slow due to its larger size (namely with negligible magnitude saturation levels despite a severe rate saturation effect) and a small one which has smaller excursions but is capable of inducing very fast small signal transients (namely it has negligible rate saturation levels in spite of a severe magnitude saturation effect). ○

B. Dynamic allocator design

From the point of view of the horizontal position regulation, the plant results to be strongly input redundant (see [13]), namely it is possible to find a matrix $B_\perp$ such that

$$Im\,(B_\perp) = Ker\left(\left[\begin{array}{c} B \\ D \end{array}\right]\right) \neq \{0\}, \tag{5}$$

therefore representing a basis of the kernel in (5).

Generalizing the approach in [13], a dynamic allocator can be designed as follows, as represented in Figure 5

$$g = -\rho B_\perp^T W(t, u_a)(u_a - u_r), \tag{6a}$$

$$\dot{\delta} = \bar{\sigma}_{MR}(\delta, g), \tag{6b}$$

$$y_a = B_\perp \delta, \tag{6c}$$

where u_a is the input to the allocator block and u_r is the desired reallocated value for this input. Moreover $\bar{\sigma}_{MR}(\cdot,\cdot)$ is a set-valued map defined as

$$\bar{\sigma}_{MR}(x, u) = \begin{cases} \sigma_R(u), & |x| < M, \\ \overline{\text{co}}\left(\{\sigma_R(u), -R\,\text{sgn}\,(x)\}\right), & |x| = M, \\ -R\,\text{sgn}\,(x), & |x| > M, \end{cases} \tag{7}$$

where $\sigma_R\,(x) = \text{sgn}\,(x)\min\left(|x|\,,|R|\right)$ is the saturation function, $\overline{\text{co}}\,(\cdot)$ is the convex hull of a set, ρ, M and R are positive scalars and $W(\cdot)$ is a weight square matrix described below. Equation (6b) represents a saturated integrator with rate saturation (see Figure 5) namely an integrator whose state can only grow up to a certain saturation level with a limited velocity. The allocator (6) is interconnected to the closed-loop as shown in Figure 4, via the equations:

$$u_a = u = \left[\begin{array}{c} i_V \\ i_F \end{array}\right], \tag{8a}$$

$$u_r = \left[\begin{array}{c} i_{V_r} \\ i_{F_r} \end{array}\right], \tag{8b}$$

$$u = y_c + y_a, \tag{9}$$

namely the input signal to the allocator u_a is the same one that enters the plant: the poloidal currents, while the reference signal u_r represents their desired values requested from the allocator. Equation (6c) together with interconnection (9) ensures that the allocator contribution belongs to the input space kernel so that no changes to the plant input u will be visible on the plant output $\Delta\Psi$ as compared to the configuration without the allocator. The operating point in this subspace corresponds to the allocator state δ which is given by a saturated integrator with saturation level equal to M: this element allows the designer to limit in amplitude the allocator contribution, for example for safety reasons.

The parameter R represents instead a rate saturation level for the allocator state δ and consequently for the allocator contribution y_a. This parameter can be tuned in order to ensure the feasibility of the requested currents with respect to the power supplies rate limits.

When the two saturations are not active, namely we are working in linear conditions, the parameter ρ specifies the allocator convergence speed. Due to the strong input redundancy of the plant the value for ρ can be adjusted theoretically as fast as desired even though, as confirmed by the experiments of section IV, unmodeled dynamics enforce a restriction on ρ. See, in particular, the oscillations in Figure 15 not predicted by the simulation of Figure 11.

A possible choice for $B_\perp$ is:

$$B_\perp = \left[\begin{array}{c} 1 \\ b \end{array}\right], \tag{10}$$

with $b = -\frac{k_V}{k_F}$. This particular choice is convenient because the allocator state δ corresponds to the i_V current variation Δi_V so that the parameters M and R are, respectively, a magnitude and a rate limit on the slow actuator contribution.

The matrix $W(t,u_a) = \begin{bmatrix} w_V(t,u_a) & 0 \\ 0 & w_F(t,u_a) \end{bmatrix} \geq 0$ is chosen with $\max(w_V, w_F) > 0$ for all pairs (t, u_a). With constant references and if a constant matrix $W = \begin{bmatrix} w_1 & 0 \\ 0 & w_2 \end{bmatrix} \geq 0$ is used, the steady state reallocated input is the one that minimizes the cost function $J(t,u_a) = (u_a - u_r)^T W (u_a - u_r)$ subject to the constraint $u_a = y_c + B_\perp \delta$, so, using the vector (w_1, w_2), it is possible to decide (see Remarks 2 and 3 in [13]) which error to penalize more; in particular if the weight of one input is equal to zero, then the other input will asymptotically reach the reference value.

The goal in this application is to make the i_F current follow a desired reference signal, while there is no interest in making the i_V current follow a particular one. For this reason it is possible to exploit the weight function in order to obtain a smooth activation mechanism for the allocator. By choosing $i_{V_r} = i_{V_c}$, if $w_F(t,u) = 0$ then the allocator effort is directed towards minimizing its own contribution and asymptotically shut down; on the other hand if $w_V(t,u) = 0$ then the allocator effort is directed towards regulating the i_F current to the reference value. In summary taking

$$W(t,u_a) = \begin{bmatrix} 1 - w_F(t,u_a) & 0 \\ 0 & w_F(t,u_a) \end{bmatrix} \tag{11}$$

with $0 \leq w_F(t,u_a) \leq 1$ for all pairs (t,u_a), allows to choose when the allocator must track the i_F current reference and when it must shut down: this can be chosen depending both on time and on the input, if there are some conditions under which the allocator must give no contribution at certain times.

A possible choice for $w_F(t,u)$ is:

$$w_F(t,u) = \gamma(u_2) r_{ON}(t) \tag{12}$$

where $r_{ON}(t)$ is an activation external signal to turn on and off the allocator at different times, satisfying $0 \leq r_{ON}(t) \leq 1$ for all times, while $\gamma(\cdot)$ can be chosen as the following trapezoidal function

$$\gamma(x) = \begin{cases} 0 & x \leq x_1, \\ \dfrac{x - x_1}{x_2 - x_1} & x_1 < x \leq x_2, \\ 1 & x_2 < x \leq x_3, \\ \dfrac{-x + x_4}{x_4 - x_3} & x_3 < x \leq x_4, \\ 0 & x_4 < x \end{cases} \tag{13}$$

with suitable choices for the parameters x_k, $k = 1, ..., 4$ and with $x_2 < 0 < x_3$. In particular these parameters can be selected in such a way that the allocator remains fully active when the i_F current is far from its saturation levels, namely in the range $[x_2, x_3]$, the allocator is fully inactive when the i_F current is outside from the range $[x_1, x_4]$, while it gradually shuts down when the i_F current is in the intermediate ranges $[x_1, x_2]$ and $[x_3, x_4]$.

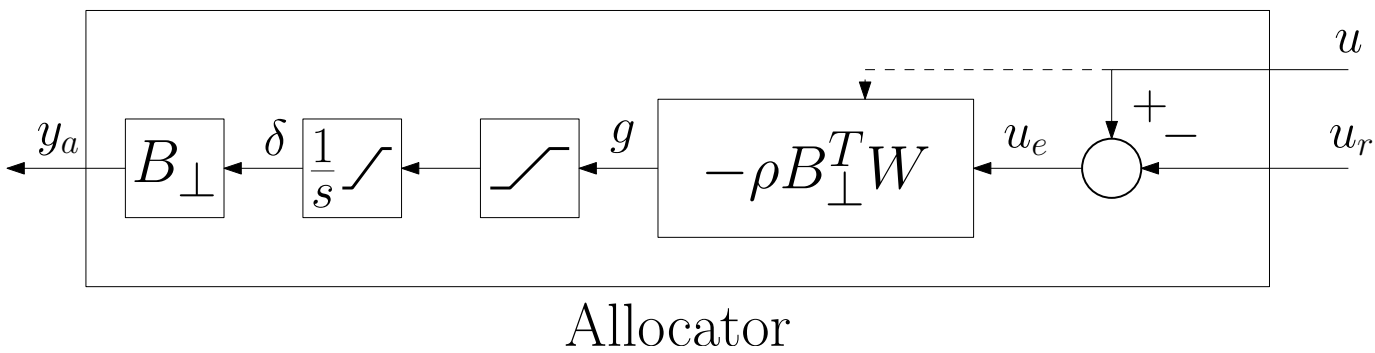

Fig. 5. Block diagram of the allocator block in Figures 4 and 7.

The following theorem gives formal guarantees about some desirable properties of the closed loop system with the allocator: in particular item (i) ensures that the allocation is transparent as far as the system output and state response is concerned; item (ii) ensures that the allocation is performed with a bounded rate which can be chosen by the designer (thus avoiding that neglected high frequency dynamics get excited by an excessively fast allocation); items (iii), (iv) and (v) ensure that the current i_F converges to a desirable value (which depends on the current operating region of the system and on the activation signal $r_{ON}(t)$ establishing whether i_F should be regulated primarily for performance or for safety).

Theorem 1: Consider the closed-loop system with input allocation given by (1), (3), (4a), (6), (8) and (9). If Assumption 1 is verified, the system has the following properties:

i) Given any initial condition $x(0), x_c(0), \delta(0)$ and any selection of $r(\cdot)$, $d(\cdot)$, $u_r(\cdot)$, the plant output y of the system and that of the system without input allocation (given by (1), (3), (4) coincide at all times.

ii) The allocator state response is limited in rate, namely $|\dot{\delta}(t)| \leq R$ at almost all times. Moreover, the set $\mathcal{M} := \{\delta : |\delta| \leq M\}$ is forward invariant and any initial state δ_0 outside $\mathcal{M}$ converges to $\mathcal{M}$ after the finite time $\frac{|\delta_0|-M}{R}$.

Moreover, if $r_{ON}(t) = 1$, $\forall t$, then:

iii) if $x_2 < i_{F_c} + bM \leq i_{F_c} - bM < x_3$ then the allocator has a globally asymptotically stable equilibrium point in $\bar{\delta} = \sigma_M\left(\frac{i_{F_r}-i_{F_c}}{b}\right)$. Moreover if $|i_{F_r} - i_{F_c}| < |b|\, M$ then $\bar{\delta}$ is locally exponentially stable and the current i_F converges to the reference value i_{F_r}; otherwise $\bar{\delta}$ is reached in finite time;

iv) if $i_{F_c} - bM < x_1$ or $i_{F_c} + bM > x_4$ then the allocator has a globally asymptotically, locally exponentially stable equilibrium point in $\bar{\delta} = 0$ and the current i_F converges to the linear controller output i_{F_c}.

Finally, if $r_{ON}(t) = 0$, $\forall t$, then:

v) the allocator has a globally asymptotically, locally exponentially stable equilibrium point in $\bar{\delta} = 0$ and the current i_F converges to the linear controller output i_{F_c}.

Proof: From the choice (5) of the matrix $B_\perp$ it follows that the allocated closed-loop system is equivalent to the cascade of two systems: the non allocated closed-loop system and the allocator system (6). So the output y of the non allocated closed-loop system is completely independent from the allocator behavior, proving point (i).

Point (ii) directly follows from the definition of the set-valued map (7), because for every pair of values of the arguments, all the elements $y \in \bar{\sigma}_{MR}(x, u)$ satisfy $|y| \leq R$.

To prove point (iii), two situations must be considered. If $|i_{F_r} - i_{F_c}| < |b|\, M$ then the equilibrium $\bar{\delta}$ is given by $\bar{\delta} = \frac{i_{F_r}-i_{F_c}}{b}$ and the function $V(\delta) = \frac{1}{2}\left(\delta - \bar{\delta}\right)^2$ is a Lyapunov function. Indeed its Lyapunov derivative is given by: [1]

$$\dot{V} \in \begin{cases} \{\left(\delta - \bar{\delta}\right)\sigma_R(-\rho b^2\left(\delta - \bar{\delta}\right))\}, & \left|\delta - \bar{\delta}\right| < M, \\ \mathrm{Co}\{\left(\delta - \bar{\delta}\right)\sigma_R(-\rho b^2\left(\delta - \bar{\delta}\right)), & \\ \qquad \left(\delta - \bar{\delta}\right)(-R\,\mathrm{sgn}\,(\delta))\}, & \left|\delta - \bar{\delta}\right| = M, \\ \{\left(\delta - \bar{\delta}\right)(-R\,\mathrm{sgn}\,(\delta))\}, & \left|\delta - \bar{\delta}\right| > M, \end{cases} \tag{14a}$$

$$= \begin{cases} \{-\rho b^2\left(\delta - \bar{\delta}\right)^2\}, & \left|\delta - \bar{\delta}\right| < \hat{M}, \\ \mathrm{Co}\{-\rho b^2\left(\delta - \bar{\delta}\right)^2, -R\left|\delta - \bar{\delta}\right|\}, & \left|\delta - \bar{\delta}\right| = \hat{M}, \\ \{-R\left|\delta - \bar{\delta}\right|\}, & \left|\delta - \bar{\delta}\right| > \hat{M}. \end{cases} \tag{14b}$$

with $\hat{M} := \min\{M, \frac{R}{\rho b^2}\}$ and it results to be negative definite. Finally if $\left|\bar{\delta}\right| < M$ then in a neighborhood of the equilibrium point $\bar{\delta}$, the condition $\dot{V} = -2\rho b^2 V$ is verified, so that the stability is locally exponential. Moreover note that when $\delta = \bar{\delta}$ the current i_F results to be $i_F = b\bar{\delta} + i_{F_c} = b\frac{i_{F_r}-i_{F_c}}{b} + i_{F_c} = i_{F_r}$.

In the second situation, if $i_{F_r} - i_{F_c} \geq |b|\, M$ the equilibrium point $\bar{\delta}$ is given by $\bar{\delta} = M$ (while it is $\bar{\delta} = -M$ if $i_{F_r} - i_{F_c} \leq -|b|\, M$, in which case the reasoning is the same). Consider the time derivative of the state, given by

$$\dot{\delta} \in \begin{cases} \{\sigma_R\left(-\rho b^2\left(\delta - \frac{i_{F_r}-i_{F_c}}{b}\right)\right)\}, & \delta < M, \\ \mathrm{Co}\{\sigma_R\left(-\rho b^2\left(\delta - \frac{i_{F_r}-i_{F_c}}{b}\right)\right)\}, & \delta = M, \\ \{-R\,\mathrm{sgn}\,(\delta)\}, & \delta > M. \end{cases} \tag{15}$$

and note that there exist $c > 0$ such that for $\delta < M$ it holds that $\dot{\delta} \geq c > 0$, while for $\delta > M$ it holds that $\dot{\delta} \leq -R < 0$. So the state converges in finite time to $\bar{\delta} = M$.

Under the assumptions of point (iv), the function $V(\delta) = \frac{1}{2}\delta^2$ is a Lyapunov function. Indeed the Lyapunov derivative is given by

$$\dot{V} \in \begin{cases} \{\delta\sigma_R(-\rho\delta)\}, & |\delta| < M, \\ \mathrm{Co}\{\delta\sigma_R(-\rho\delta), \delta\,(-R\mathrm{sgn}\,(\delta))\}, & |\delta| = M, \\ \{\delta\,(-R\mathrm{sgn}\,(\delta))\}, & |\delta| > M, \end{cases} \tag{16a}$$

$$= \begin{cases} \{-\rho\delta^2\}, & |\delta| < \hat{M}, \\ \mathrm{Co}\{-\rho\delta^2, -R\,|\delta|\}, & |\delta| = \hat{M}, \\ \{-R\,|\delta|\}, & |\delta| > \hat{M}. \end{cases} \tag{16b}$$

which results to be negative definite. Moreover in a neighborhood of the origin we have $\dot{V} = -2\rho b^2 V$, so that the stability is locally exponential. The proof of point (v) parallels to that of point (iv). ■

[1] Note that in (14) and (16) we use set valued right hand sides and establish the Lyapunov result by proving that any value of $\dot{V}$ in the allowed set will satisfy the required negative definiteness bound. For more insight on Lyapunov tools and set-valued maps, the reader is referred, e.g., to [6].

C. Extension to elongation control

An important goal of this application is to obtain a slow regulation of the plasma elongation κ, defined as the ratio between the vertical and horizontal plasma length. This can be done using the allocation scheme presented in the previous section thanks to a quasi-static relationship between the elongation κ and the current i_F of the form

$$\kappa = f(i_F) \tag{17}$$

which can be approximated by the map

$$\hat{\kappa} = \hat{f}(i_F) = \kappa_0 - \kappa_1 \frac{i_F}{i_P}, \tag{18}$$

which is affine in i_F, while the current i_P can be seen as a time varying parameter. The numerical values of the parameters κ_0 and κ_1 have been estimated by a least squares fit of the experimental data, reported in Figure 6. In particular they correspond to $\kappa_0 = 1.03$ and $\kappa_1 = -4.61$.

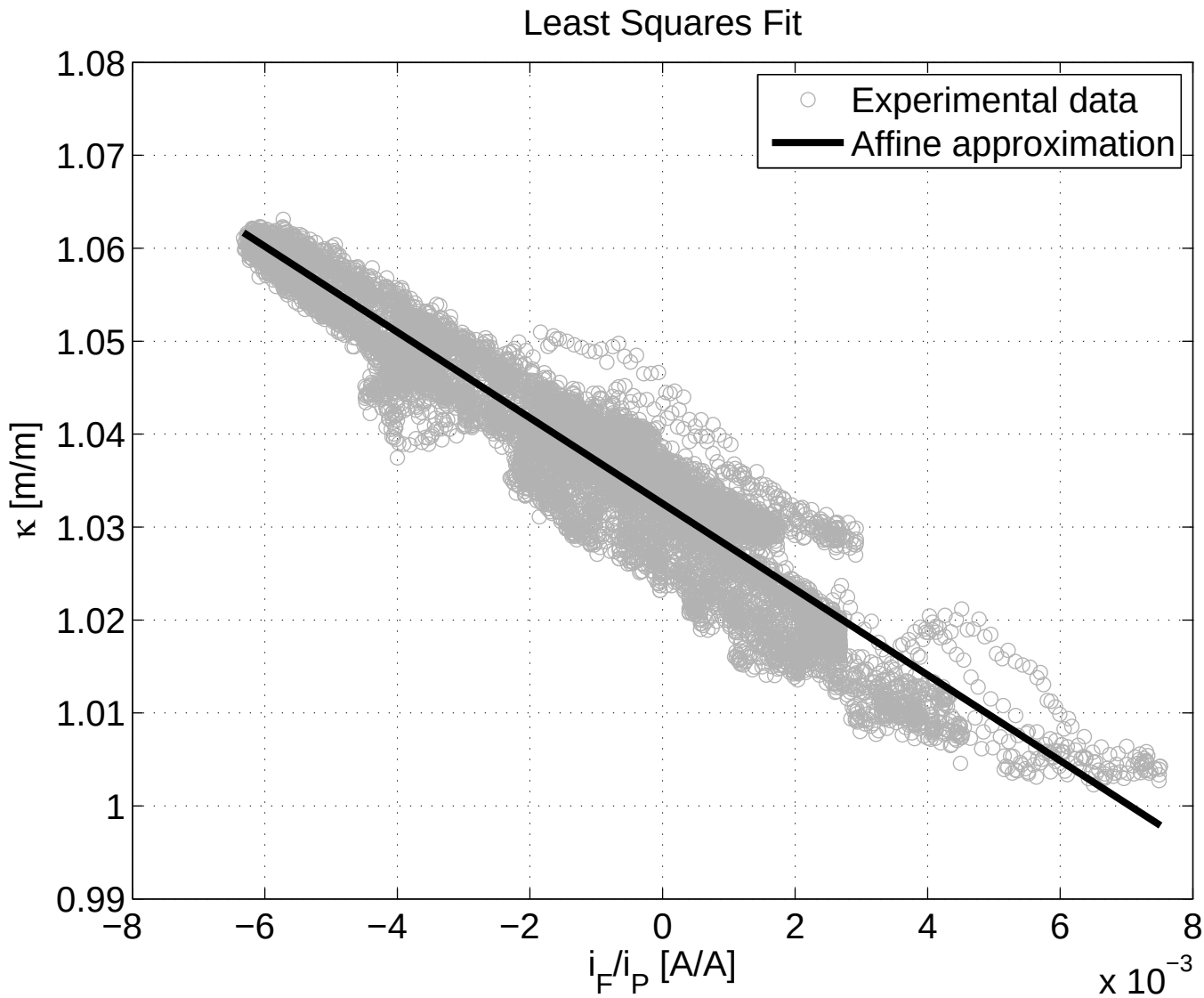

Fig. 6. Relationship between the elongation κ and the current i_F after normalizing the plasma current. Experimental data (circles) and fitted line (solid) obtained by a least squares approximation.

Since i_P is measured in real-time, the map $\hat{f}(\cdot)$ in (18) from i_F to κ can be inverted so that given a certain elongation κ, the current i_F enforcing that elongation is computed as

$$i_F = f^{-1}(\kappa) \tag{19}$$

which is approximated by

$$\hat{i}_F = \hat{f}^{-1}(\kappa) = -\frac{i_P}{\kappa_1}(\kappa - \kappa_0). \tag{20}$$

Finally the allocator inputs are chosen as

$$u_a = \begin{bmatrix} i_V \\ \hat{i}_F \end{bmatrix}, \quad u_r = \begin{bmatrix} i_{V_r} \\ \hat{i}_{F_r} \end{bmatrix}, \tag{21a}$$

$$\hat{i}_F = \hat{f}^{-1}(\kappa), \quad \hat{i}_{F_r} = \hat{f}^{-1}(\kappa_r). \tag{21b}$$

where $\hat{i}_F$ and $\hat{i}_{F_r}$ are computed using the approximate inverse of $f(\cdot)$ according to (20), using, respectively, the elongation measurement which is available in real-time and the elongation reference κ_r. The overall closed-loop is in feedback from the elongation measurement signal and is represented in Figure 7. For this scheme the following result can be proven.

Theorem 2: Consider the modified control system given by (1), (3), (4a), (6), (9), (17), (21). If in this system $\hat{i}_F$ asymptotically converges to $\hat{i}_{F_r}$, then also κ asymptotically converges to κ_r.

Proof: If $i_F = i_{F_r}$, from the choice (21b) it follows that $\hat{f}^{-1}(\kappa) = \hat{f}^{-1}(\kappa_r)$. Since the function $\hat{f}(\cdot)$ is invertible, then this is true if and only if $\hat{f}(\hat{f}^{-1}(\kappa)) = \hat{f}(\hat{f}^{-1}(\kappa_r))$, i.e. $\kappa = \kappa_r$. ■

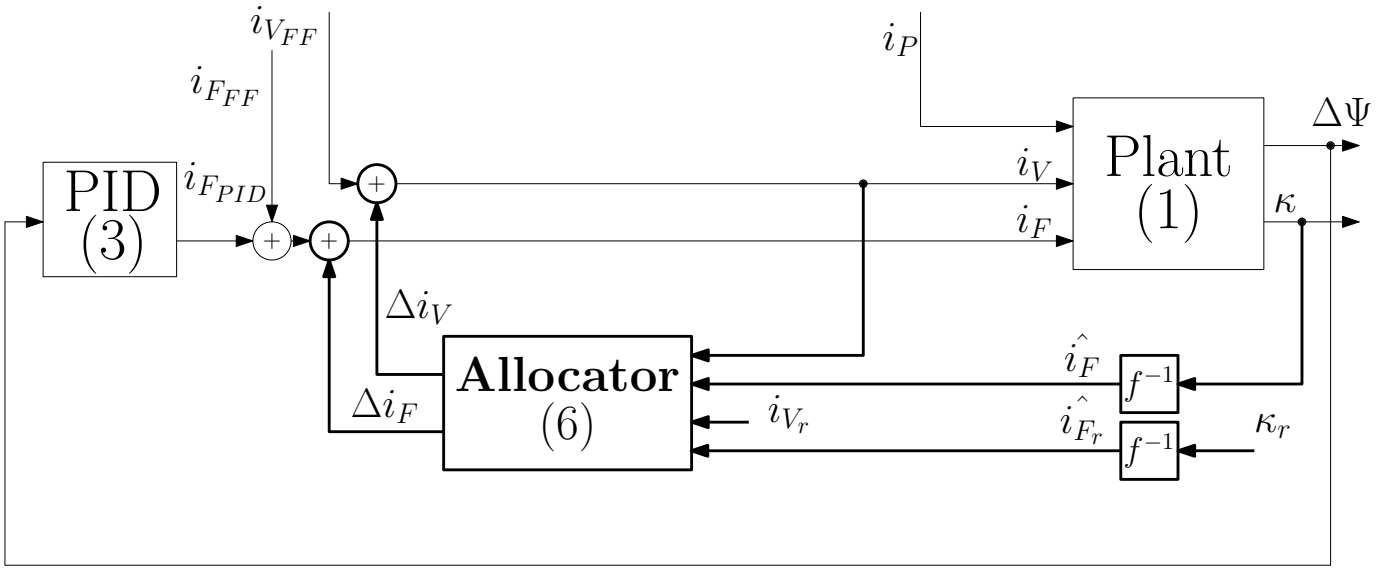

Fig. 7. Block diagram of the allocation scheme for elongation regulation.

Remark 2: The convergence property assumed in Theorem 2 trivially holds if $\hat{f} = f$ and i_{F_c}, i_{F_r} satisfy the conditions in case (iii) of Theorem 1. Then Theorem 2 shows that the convergence of κ to κ_r is still ensured if $\hat{f}$ is just an approximation of f, as long as convergence of $\hat{i}_F$ to $\hat{i}_{F_r}$ is preserved (which, by standard reasonings about small perturbations is true, provided that $\hat{f}$ is sufficiently close to f). This robustness property is similar to what is achieved in output tracking when an internal model of the reference is used, i.e. tracking is robust as long as stability is preserved. ○

III. Simulation results

In this section some simulation results are presented to illustrate how the allocator works and how the different parameters can be tuned. In all the simulations, the parameters of model (1) are selected as: $k_P = -1.12e^{-8}$, $k_V = -1.18e^{-6}$, $k_F = -2.75e^{-7}$, $\tau = 8e^{-3}$. To reproduce the experimental scenario of FTU, the PID controller is implemented by the discrete-time transfer function

$$\frac{i_{F_{PID}}(z)}{\Delta\Psi(z)} = -k_p - k_i\frac{T_s}{2}\frac{z+1}{z-1} - k_d\frac{z-1}{(\tau_d + T_s)z - \tau_d} \tag{22}$$

where $Ts = 5e^{-4}$ is the sampling time, $\tau_d = 4e^{-3}$. According to the configuration of the FTU control system, the PID gains are not constant, but first ramp up from zero to the steady-state values $k_p = 7.5e^3$, $k_i = 1e^6$ and $k_d = 22.5$ in the time intervals $[0, 0.05]$, $[0, 0.16]$ and $[0, 0.02]$, respectively; then they remain constant and finally ramp down to zero in the time intervals $[1.6, 2]$, $[1.6, 2]$ and $[1.6, 1.8]$, respectively. The overall linear controller action is given by

$$y_c = \begin{bmatrix} i_{V_{FF}} \\ i_{F_{FF}} + i_{F_{PID}} \end{bmatrix}. \tag{23}$$

The activation signal $r_{ON}(\cdot)$ is chosen as a trapezoidal shape to activate the allocator at $0.4s$ when the ramp-up phase is finished and smoothly shut down during the time window $[1.4s, 1.5s]$ (see the upper plot in Figure 8).

In the first simulation, as shown by the dash-dotted curves in the middle plots of Figure 8 the input signals for the closed-loop model $i_{V_{FF}}$, $i_{F_{FF}}$ and i_P have a trapezoidal shape: $i_{V_{FF}}$ ramps up from 0 and reaches 4938.9 at time 0.2585, then ramps up to 4945 at time 1.5, and finally ramps down to 0 at time 1.8; $i_{F_{FF}}$ jumps to 2000 at time 0, then ramps up to 2500 at time 1.5, and finally ramps down to 0 at time 1.7; i_P ramps from 0 up to $-5e^5$ at time 0.148, then is constant until time 1.5, and finally ramps down to 0 at time 1.8. The reference i_{F_r} driving the allocator is the piecewise constant signal corresponding to the dashed curve in the middle-top plot of Figure 8.

The same simulation is repeated with the allocator working in current mode, i.e. with a i_F current reference, and without the allocator. In Figure 8 the plant inputs and outputs are shown. The two simulations appear the same up to time $0.4s$ when the allocator is turned on and starts modifying the inputs in order to regulate the current i_F to the reference value. It is evident that, while the input signals are different in the two simulations, the plant outputs $\Delta\Psi$ are perfectly superimposed in the two simulations, showing that the allocator is invisible from the plant output.

When large instantaneous excursions are requested from the allocator, for example at time $0.8s$, the rate saturation effect is evident in the first part of the transient, while in the second part of the transient, when the difference between i_F and i_{F_r} is smaller, the exponential convergence appears. All the i_F variations requested by the allocator, can also be seen on the i_V current request, suitably scaled.

In order to observe how the shut down mechanism works, the same simulation is repeated in Figure 9 with more stringent values of the weight function parameters, namely $x_3 = 3500$ and $x_4 = 3700$, and with a current reference i_{F_r} which requests the allocator to bring the current i_F in a forbidden region. When i_F passes through the boundary zone $[x_3, x_4]$, the weight w_F decreases so that the allocator is almost shut off. As a consequence, in that part of the simulation, the reference signal is not tracked. After time $1.15s$, the allocator is requested to drive the current i_F back inside the allowed interval and the reference signal is tracked again. At time $1.4s$, since we are close to the end of the pulse, the weight w_F is decreased by the decreasing activation signal $r_{ON}(\cdot)$ for the final shut-off and this limits again the allocator's authority.

A third simulation is presented in Figure 10, showing the allocator working in elongation mode. The input signals $i_{V_{FF}}$, $i_{F_{FF}}$ and i_P have the following trapezoidal shapes: $i_{V_{FF}}$ ramps from 0 up to -4940 at time 0.3, then sits at -4945 up to time 1.5, and finally ramps down to 0 at time 1.8; $i_{F_{FF}}$ ramps from 0 up to -1500 at time 0.14, then sits at -1500 up to time 1.5, and finally ramps down to 0 at time 1.7; i_P ramps from 0 up to $-5e^5$ at time 0.25, then sits at $-5e^5$ up to time 1.5, and finally ramps down to 0 at time 1.8. The elongation reference κ_r is a piecewise constant signal.

The same simulation is repeated with different values of ρ, respectively $\rho = 7$, $\rho = 1$ and $\rho = 0.5$, to show how this affects the allocator convergence speed (see Figure 11). It is evident that increasing ρ the convergence speed increases too; at the same time, the rate saturation effect becomes more evident.

IV. Experimental results

The dynamic allocation algorithm has been implemented in the FTU control system and tested during a series of experimental shots. Some experiments are presented in this section showing the allocator working both in current and elongation control mode. For the experiments reported below, the important parameters involved n the tuning of the allocator dynamics (6), (7), (10), (8), (9), (11), (12), (13) (as well as their extension to elongation control) correspond to:

- the activation signal $r_{ON}(t)$, which selects the time window where the allocator should be active; it has been chosen using the profile in the top plot of Figure 8;
- the allocator gain ρ, which allows to tune the speed of operation of the allocator dynamics, thereby ensuring that unmodeled dynamics are not excited (see Figure 15);
- the maximum allocator rate R, ensuring that the rate requested to the (rate saturated) V coil is well below the physical limits; it has been chosen as $5000A/s$;
- the maximum magnitude levels x_1, x_2, x_3, x_4 allowed for the F current, which enforce a limit on the allowable current enforced by the allocator on the F coil; they have been chosen as $(x_1, x_2, x_3, x_4) = (-6, -5, 5, 6)kA$ but were never activated in the experiments (namely, the function $\gamma(\cdot)$ in (13) was always equal to 1).

The above parameters are the main knobs available to the design engineer and correspond to tunable parameters of the elongation controller currently operating at FTU.

A. Current control

Two experiments are presented with the allocator working in current mode: the allocator tracks a reference signal for i_F, modifying the current i_V in order to maintain the horizontal plasma position unchanged. The two shots have different i_F current references and different operating conditions. Instead the allocator parameters are the same in both the experiments: the allocator gain is $\rho = 7$, while a saturation value of $5000A/s$ is imposed on the allocator state rate $\dot{\delta}$ (which corresponds to the maximum i_V current rate, thanks to the specific choice of $B_\perp$ in (ii)). Mimicking the top plot of Figure 10, the activation signal r_{ON} is zero up to time $0.4s$, one up to time $1.4s$, then linearly ramps down to zero in the time window from $1.4s$ to $1.5s$. This choice ensures that the allocator is fully active only during the flat top phase and then smoothly shuts down.

Shot number 31725 in Figure 12 reproduces experimentally the same test made in the simulation of Figure 8, namely the same input signals are used: a piecewise constant reference is requested for the current i_F jumping from $3000A$ to $2000A$

and again to $3000A$ (see top plot). From time $0.4s$, when the allocator is activated, the current i_V (solid curve in the middle plot) is moved away from its preprogrammed feedforward value (dash-dotted curve in the middle plot) in order to track the i_F current reference value of $3000A$. The rate saturation effect is evident in the solid V current trace of the middle plot around times 0.8 and 1.1, when the reference instantaneously jumps from $3000A$ to $2000A$ and viceversa. The rate saturation inside the allocator prevents it from generating an infeasible request from the power supply. Despite the deviations of the currents in the F and V coils from the preprogrammed feedforward values, the output signal $\Delta\Psi$ (lower plot) is unaffected by the large input excursions.

Shot 31855 is shown in Figure 13, where the preprogrammed feedforward $i_{V_{FF}}$ current has a peculiar profile, presenting a bump between times $0.3s$ and $0.9s$. The reference is again piecewise constant, but jumping from $-2000A$ to $0A$ and finally to $-3000A$ (see top plot). When the allocator is activated at $t = 0.4$, the current i_F ramps down to the reference value at the maximum admissible rate and reaches $-2000A$ just in time to ramp up towards the new $0A$ reference value, where it remains up to time $0.85s$, when it begins to ramp down again to reach $-3000A$. This second ramp down starts before the i_F reference changes due to the variations of the preprogrammed feedforward $i_{F_{FF}}$ and $i_{V_{FF}}$ currents (see the dash-dotted curves in the two upper plots). Also in this second case of Figure 13 the output $\Delta\Psi$ is not affected by the allocator. Indeed note that the two peaks at times $0.3s$ and $0.9s$ are not caused by the allocator but by the ramps in the preprogrammed feedforward $i_{V_{FF}}$ current signal representing a disturbance for the PID controller.

B. Elongation control

Various experiments are presented in this section to show the allocator working in elongation mode: the allocator changes the i_F current in order to track an elongation reference signal while adjusting the i_V current in order to keep $\Delta\Psi$ unchanged. This is accomplished using the scheme presented in Section II-C in feedback from the real-time elongation measurement and mimicking the simulations of Figures 10 and 11.

In shot 31971, shown in Figure 14, the test made in the simulation of Figure 10 is experimentally reproduced: the elongation reference signal is piecewise constant and jumps from 1.04 to 1.06, then to 1.03 and finally again to 1.04. Shot 31970 is an identical experiment with the allocator deactivated. It is shown in the same picture in order to underline the allocator contribution.

In the top plot of Figure 14, the real-time elongation measurement is shown to track the reference when the allocator is active (shot 31971, from time $0.4s$). In the same plot, shot 31970 shows the elongation response without the allocator contribution. The lower plots show how the allocator changes the currents in the F and V coils in order to obtain the desired elongation and to leave the radial position unchanged.

In shots 31937 and 31975, reported in Figure 15, the same experiment is repeated with different values for the allocator gain ρ. In particular while in shot 31971 we use $\rho = 1$, in shot 31937 we use $\rho = 7$ and in shot 31975 we use $\rho = 0.5$ (the same values tested in the simulations of Figure 11). Figure 15 shows a comparison of the three shots, revealing that when ρ becomes too large, the allocator becomes too aggressive with respect to some neglected plant dynamics and/or delay, thus destabilizing the closed-loop. Indeed, in the experiment with $\rho = 7$, the elongation response exhibits persistent oscillations. Also note that, as correctly predicted by the simulation of Figure 11, when $\rho = 0.5$ the allocator is quite slow and the elongation has not enough time to reach the setpoint value. The best results are obtained for $\rho = 1$. The same effects can be better appreciated on the current i_V because of the presence of noise on the elongation measurement. It is interesting to observe that the oscillations generated with $\rho = 7$ are not present in the simulation results of Figure 11; they are also not present in shot number 31725 when the allocator has the same value for ρ but it works in current mode. This suggests the presence of some neglected dynamics in the nonlinear relationship between the elongation and the current i_F which is assumed to be static in (17).

V. Conclusions

In this paper we presented a dynamic allocation scheme to achieve high bandwidth horizontal position regulation and low bandwidth elongation regulation of the FTU plasma. The nonlinear solution was first shown to guarantee desirable closed-loop properties by a suitable theoretical investigation. Then, both simulation and experimental tests confirmed the effectiveness of the proposed nonlinear dynamic allocation scheme.

References

[1] M. Ariola and A. Pironti. *Magnetic Control of Tokamak Plasmas*. Springer Verlag, 2008.

[2] A.Serrani and M. Bolender. Invited session: Control of over-actuated systems: Application to guidance and control of aerospace, marine and terrestrial vehicles. In *14th Mediterranean Conference on Control and Automation*, Ancona (Italy), June 2006.

[3] L. Boncagni, S. Galeani, G. Granucci, G. Varano, V. Vitale, and L. Zaccarian. Using dynamic input allocation for elongation control at FTU. *Fusion Engineering and Design*, 85(3-4):443–446, 2010.

[4] C.T. Chen. *Linear system theory and design*. Holt Rinehart and Winston, 1984.

[5] T.I. Fossen and T.A. Johansen. A survey of control allocation methods for ships and underwater vehicles. In *14th Mediterranean Conference on Control and Automation*, Ancona (Italy), June 2006.

[6] R.A. Freeman and P.V. Kokotović. *Robust Nonlinear Control Design - State-Space and Lyapunov Techniques*. Systems & Control: Foundations & Applications. Birkhäuser Boston, USA, 1996.

[7] A. Al Mamun, I. Mareels, T.H. Lee, and A. Tay. Dual stage actuator control in hard disk drive - a review. In *IECON Annual Conference of the Industrial Electronic Society*, pages 2132–2137, Roanoke (VA), USA, November 2003.

[8] M.W. Oppenheimer, D.B. Doman, and M.A. Bolender. Control allocation for over-actuated systems. In *14th Mediterranean Conference on Control and Automation*, Ancona (Italy), June 2006.

[9] A. Pironti and M. Walker. Special issue on control of tokamak plasmas (vol 1). *IEEE Control Systems Magazine*, 25(5), 2005.
[10] A. Pironti and M. Walker. Special issue on control of tokamak plasmas (vol 2). *IEEE Control Systems Magazine*, 26(2), 2006.
[11] G. De Tommasi, S. Galeani, A. Pironti, G. Varano, and L. Zaccarian. Trading output performance for input allocation: application to the JET Tokamak shape controller. In *Conference on Decision and Control*, pages 303–308, Shanghai (China), December 2009.
[12] G. Varano, L. Boncagni, S. Galeani, G. Granucci, V. Vitale, and L. Zaccarian. Results on plasma position and elongation regulation at FTU using dynamic input allocation. In *Conference on Decision and Control*, pages 2753–2758, Atlanta (GA), USA, December 2010.
[13] L. Zaccarian. Dynamic allocation for input-redundant control systems. *Automatica*, 45:1431–1438, 2009.
[14] L. Zaccarian, L. Boncagni, D. Cascone, C. Centioli, S. Cerino, F. Gravanti, F. Iannone, F. Mecocci, L. Pangione, S. Podda, V. Vitale, and R. Vitelli. Nonlinear instabilities induced by the F coil power amplifier at FTU: modeling and control. *Fusion Engineering and Design*, 84(7–11):2015–2019, 2009.

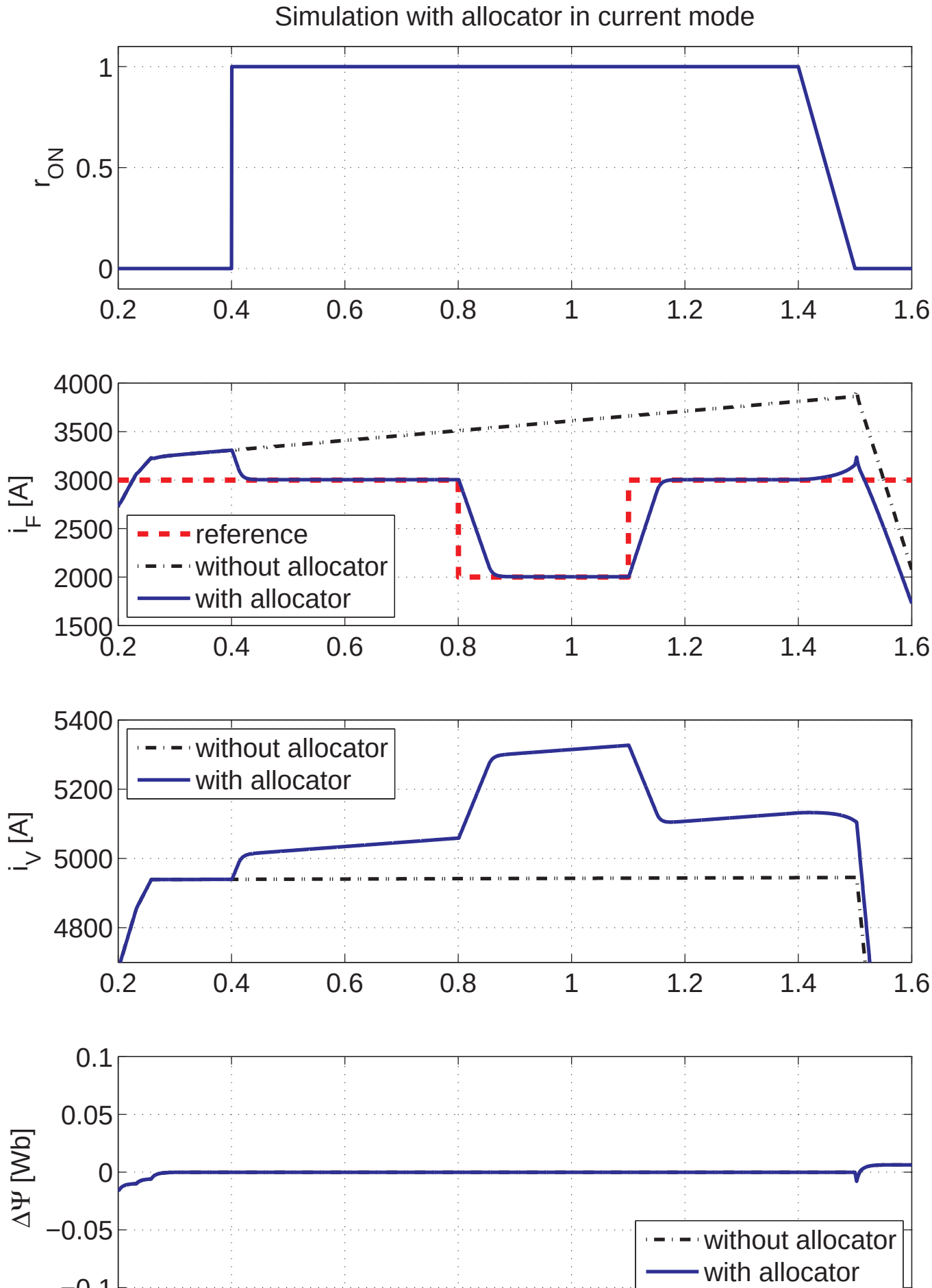
Simulation with allocator in current mode
r_ON
1
0.5
0
0.2
0.4
0.6
0.8
1
1.2
1.4
1.6
i_F [A]
4000
3500
3000
2500
2000
1500
reference
without allocator
with allocator
i_V [A]
5400
5200
5000
4800
without allocator
with allocator
ΔΨ [Wb]
0.1
0.05
0
−0.05
without allocator
with allocator

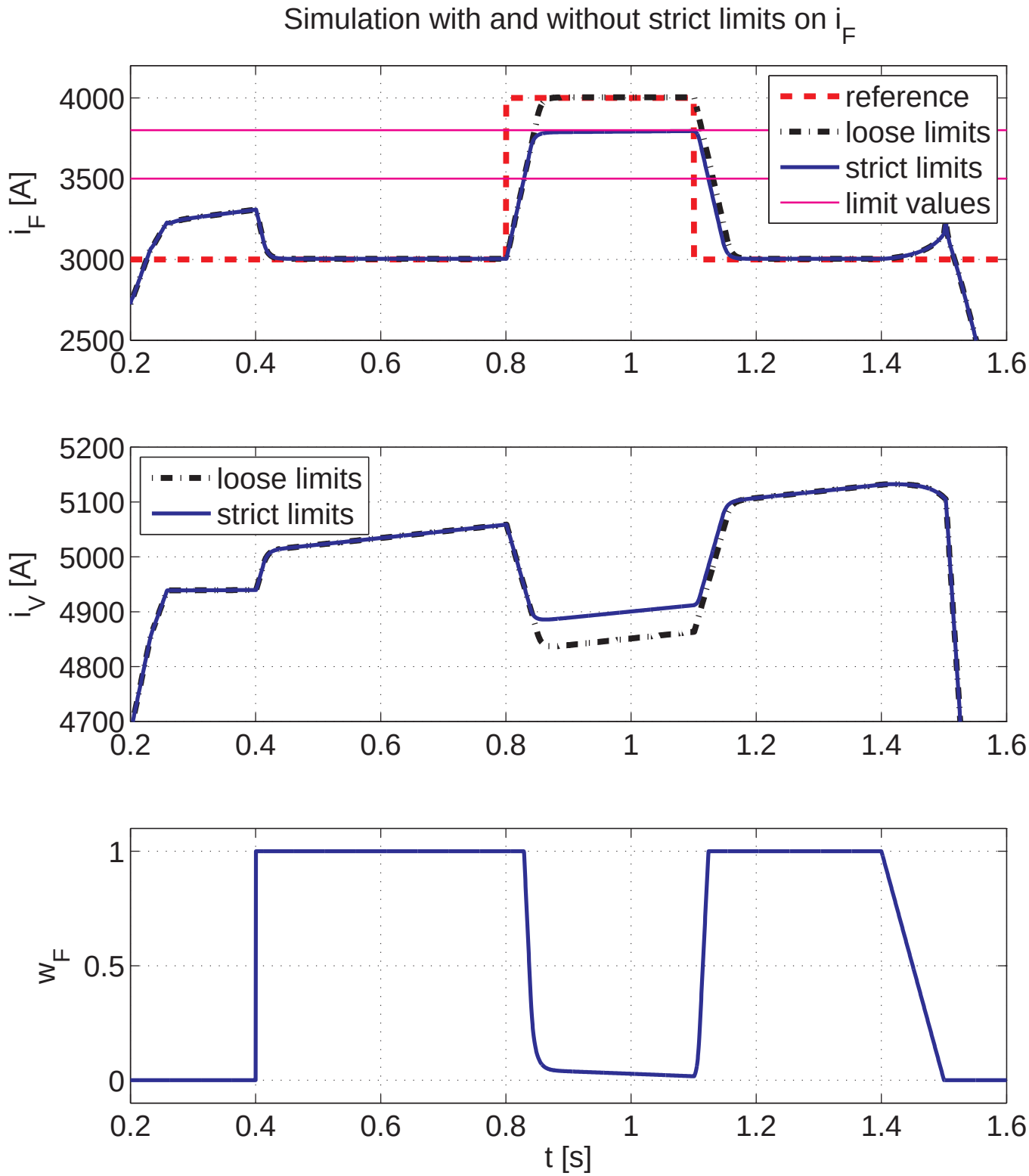

Fig. 9. Closed-loop simulation with the allocator working in current mode: without limits on i_F (dash-dotted); with strict i_F limits (solid), with a boundary zone between 3500 and 3700 (dashed). The weight w_F automatically decreases to prevent the allocator from driving i_F in the forbidden zone.

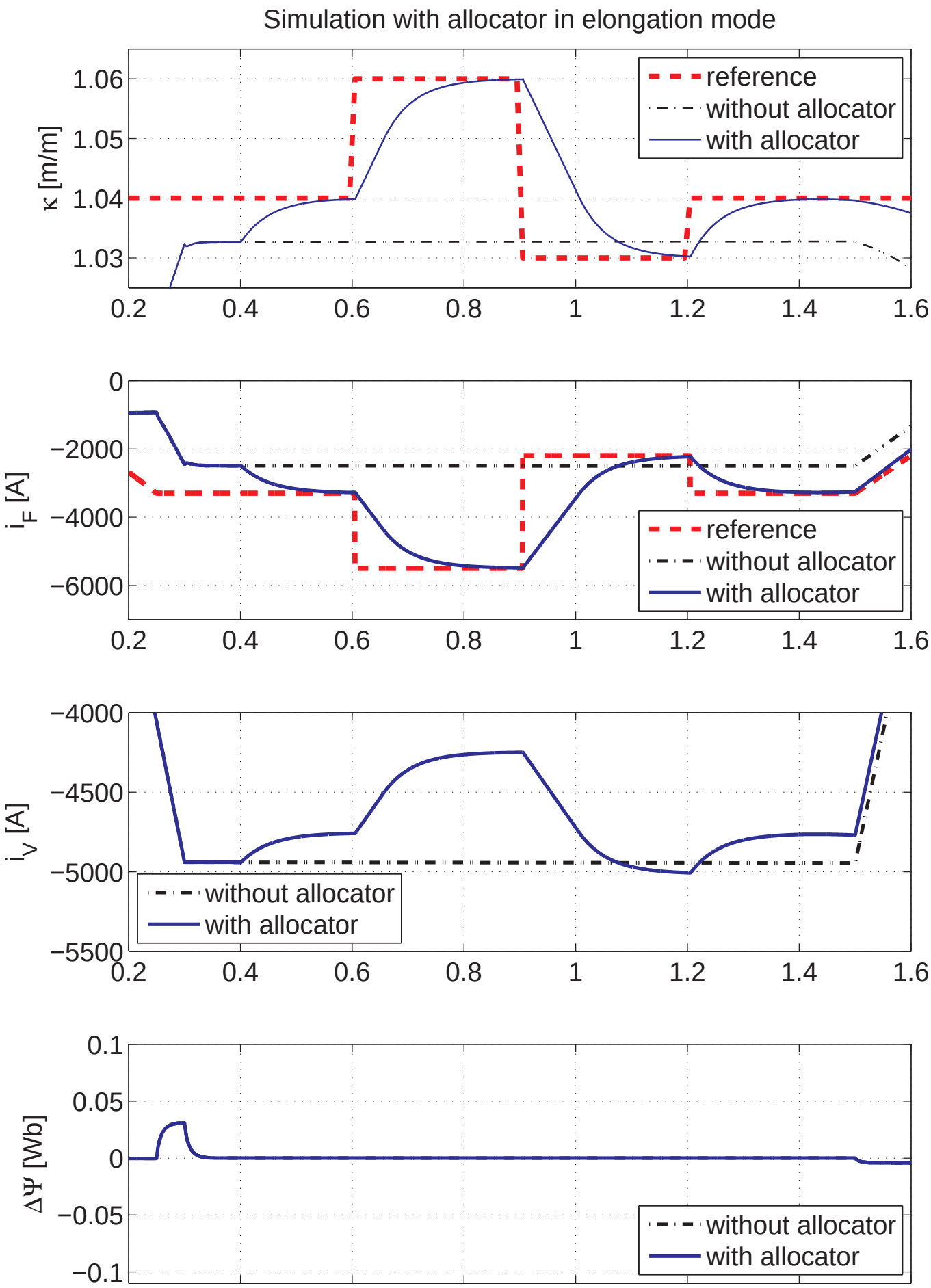
Simulation with allocator in elongation mode
κ [m/m]
1.06
1.05
1.04
1.03
0.2
0.4
0.6
0.8
1
1.2
1.4
1.6
reference
without allocator
with allocator
i_F [A]
0
−2000
−4000
−6000
reference
without allocator
with allocator
i_V [A]
−4000
−4500
−5000
−5500
without allocator
with allocator
ΔΨ [Wb]
0.1
0.05
0
−0.05
−0.1
without allocator
with allocator

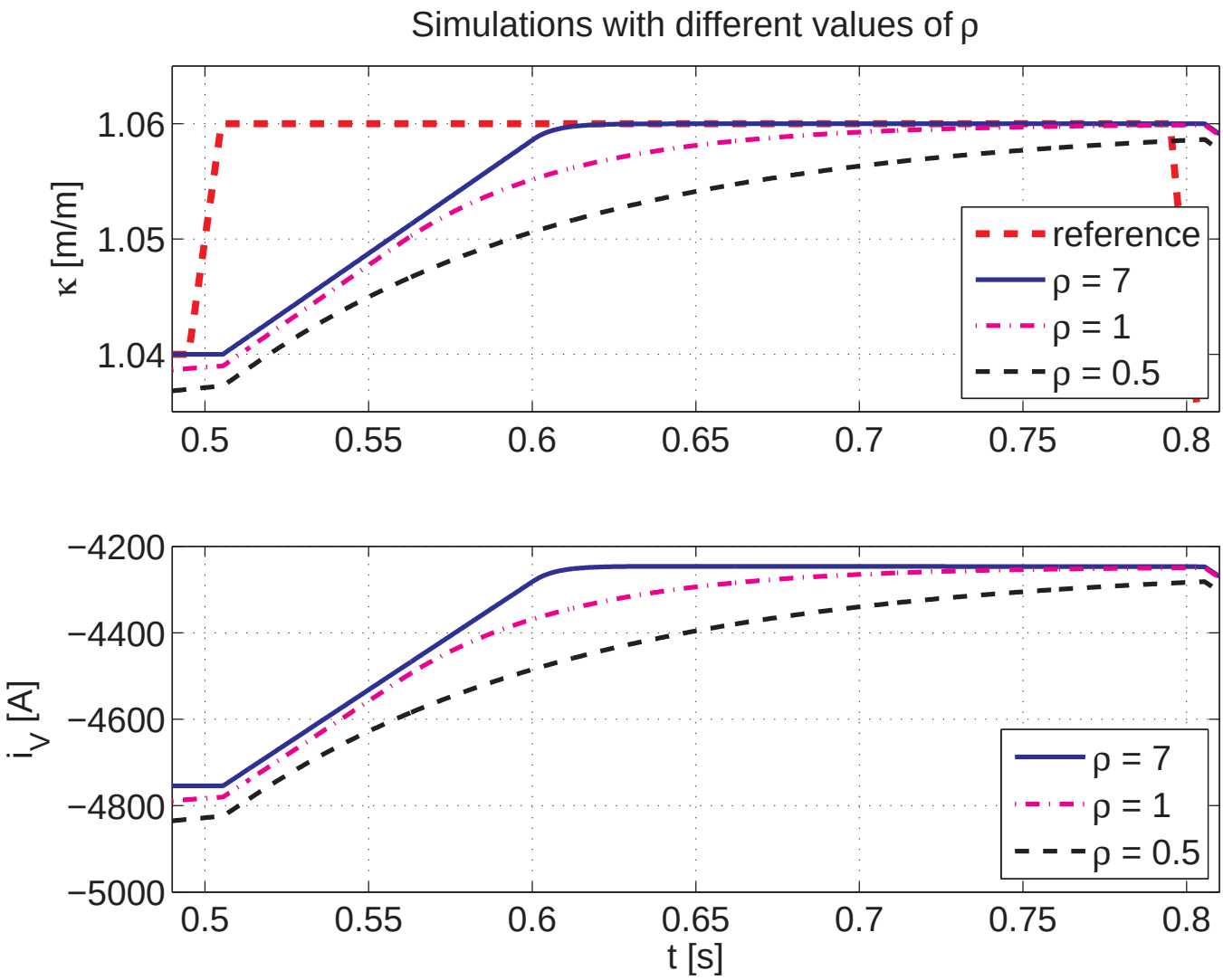

Fig. 11. Closed-loop simulations with the allocator working in elongation mode with different values of the parameter ρ: $\rho = 7$ (solid), $\rho = 1$ (dash-dotted), $\rho = 0.5$ (dashed). The greater the value of ρ, the faster the convergence to the reference value (upper light dashed) and the more the rate saturation effect is evident.

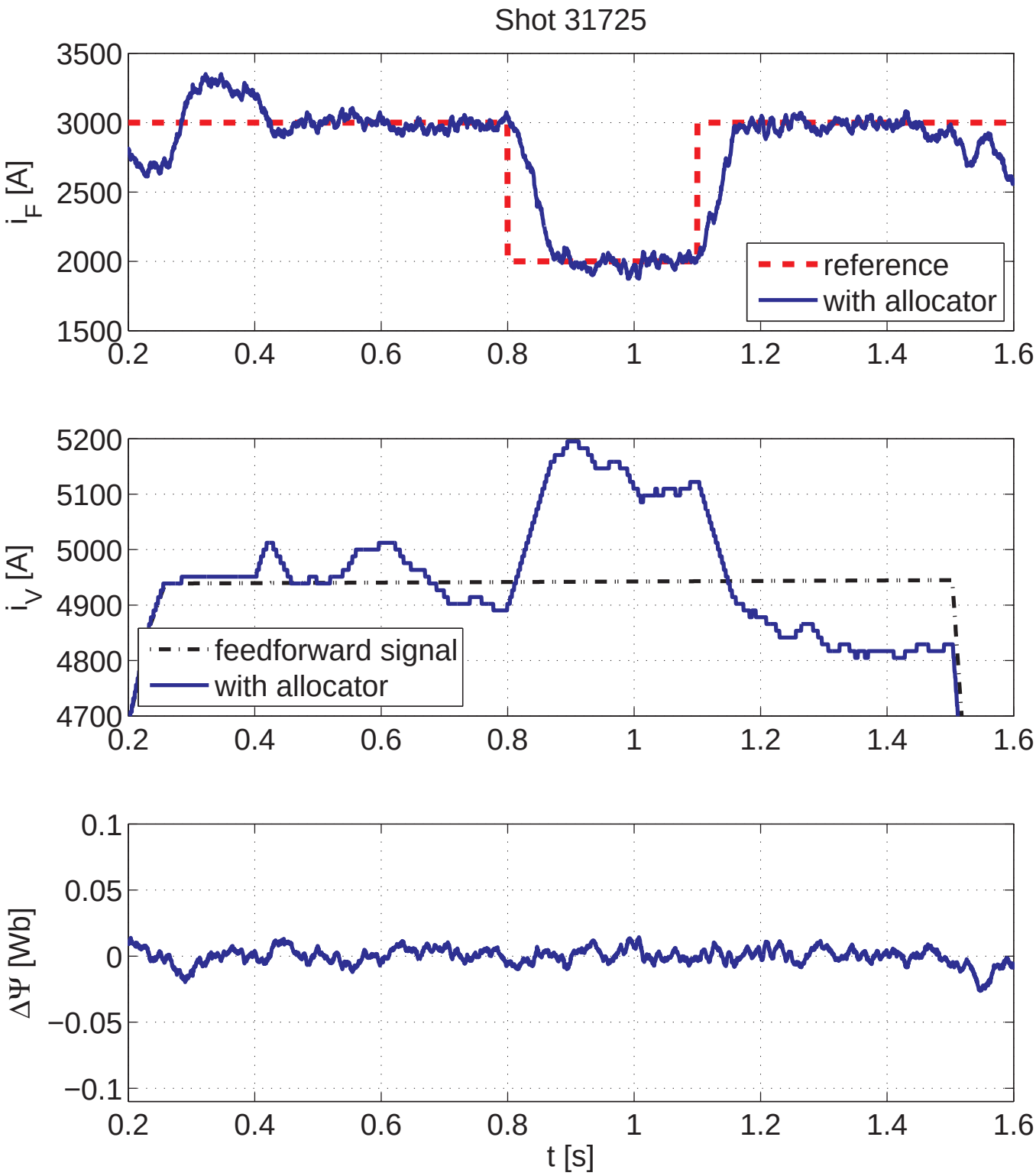

Fig. 12. Shot 31725: the current i_F (upper solid) tracks the reference (upper dashed), while the current i_V (middle solid) changes with respect to its preprogrammed feedforward value (middle dash-dotted) in order to leave $\Delta\Psi$ (lower solid) unchanged.

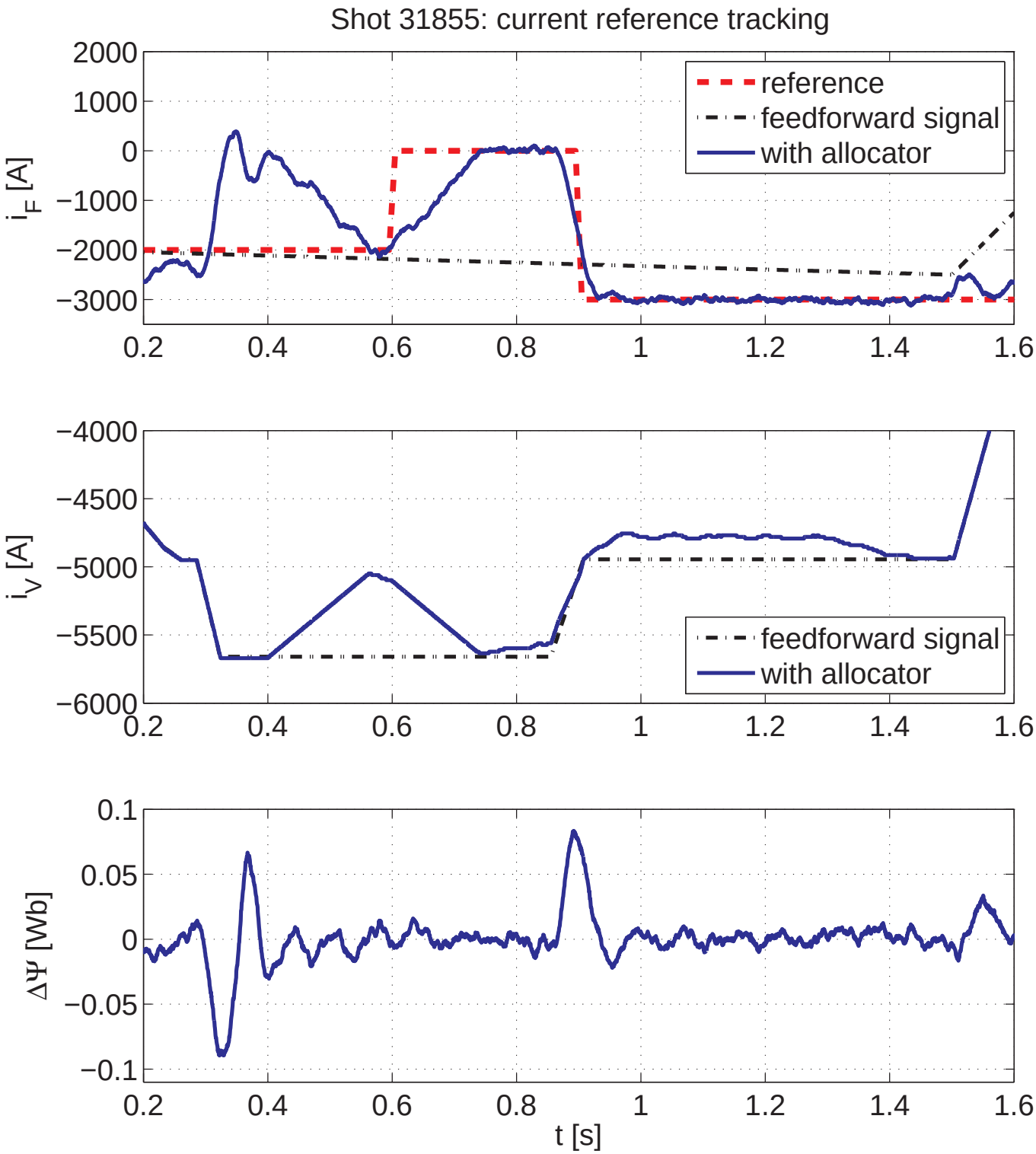

Fig. 13. Shot 31855: the current i_F (upper solid) follows the reference (upper dashed), while the current i_V (middle solid) changes with respect to its preprogrammed feedforward value (middle dash-dotted) in order to keep $\Delta\Psi$ (lower solid) unchanged.

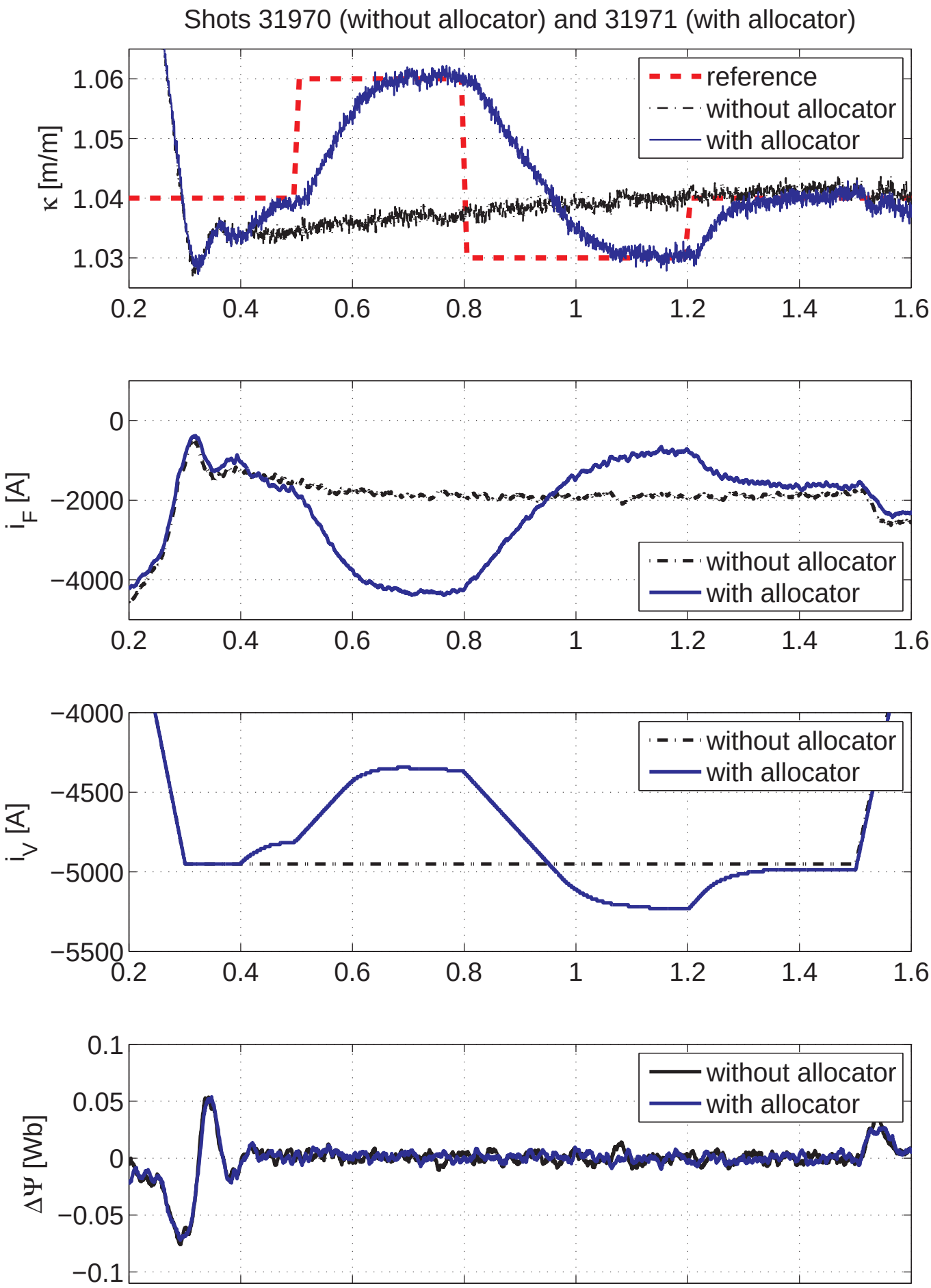
Shots 31970 (without allocator) and 31971 (with allocator)
κ [m/m]
reference
without allocator
with allocator
i_F [A]
without allocator
with allocator
i_V [A]
without allocator
with allocator
ΔΨ [Wb]
without allocator
with allocator

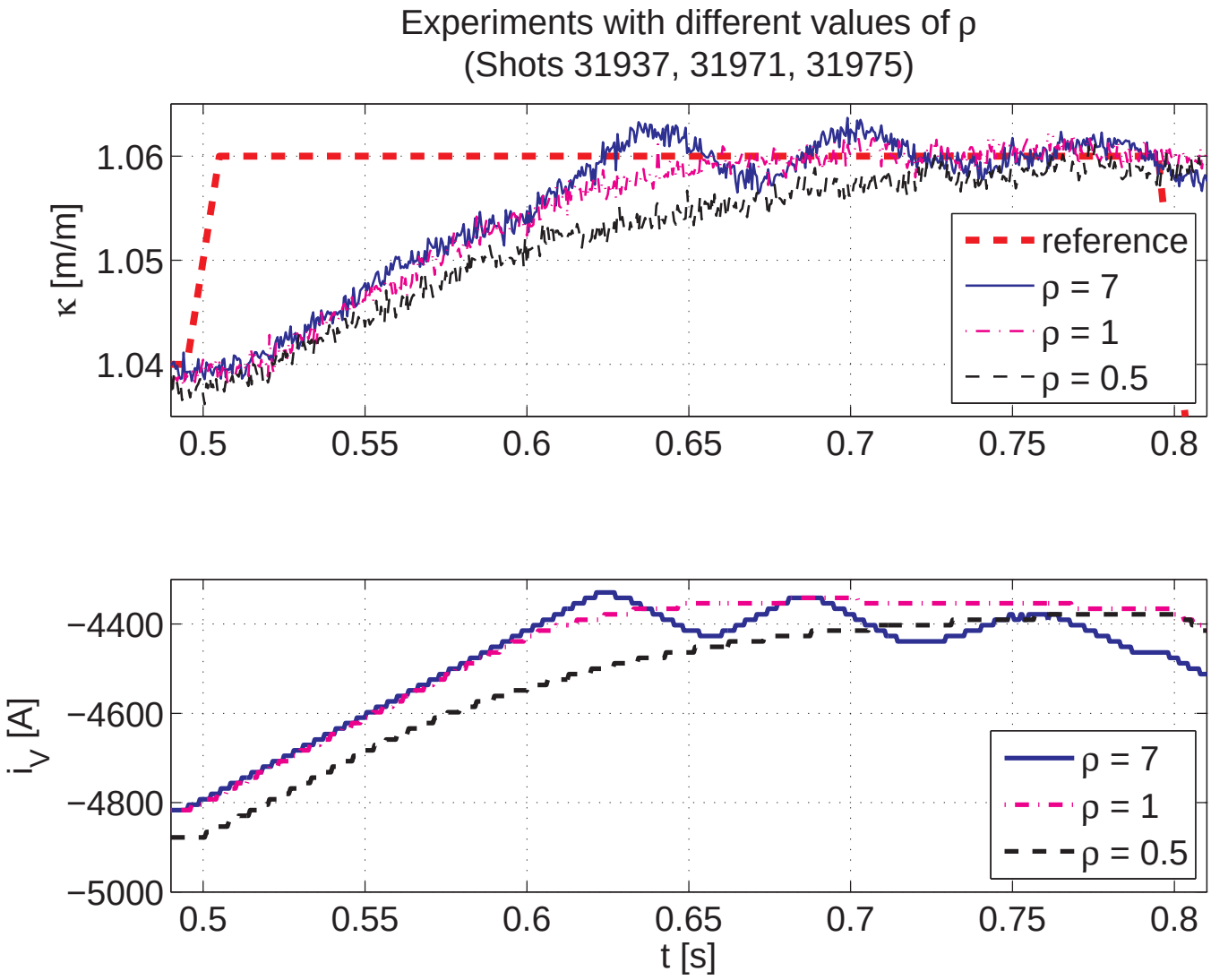

Fig. 15. Comparison of the elongation responses in shots 31937, 31971 and 31975 with the allocator working with different values of ρ (respectively 7, 1 and 0.5). With $\rho = 7$ the allocator is too aggressive and persistent oscillations occur. With $\rho = 0.5$ the allocator is too slow and the elongation reaches the setpoint too late.